

## A Crank–Nicolson scheme for the Landau–Lifshitz equation without damping

Darae Jeong, Junseok Kim\*

Department of Mathematics, Korea University, Seoul 136-701, Republic of Korea

### ARTICLE INFO

#### Article history:

Received 12 June 2009

Received in revised form 6 November 2009

#### MSC:

65Z05

#### Keywords:

Landau–Lifshitz equation

Crank–Nicolson

Finite difference method

Nonlinear multigrid method

### ABSTRACT

An accurate and efficient numerical approach, based on a finite difference method with Crank–Nicolson time stepping, is proposed for the Landau–Lifshitz equation without damping. The phenomenological Landau–Lifshitz equation describes the dynamics of ferromagnetism. The Crank–Nicolson method is very popular in the numerical schemes for parabolic equations since it is second-order accurate in time. Although widely used, the method does not always produce accurate results when it is applied to the Landau–Lifshitz equation. The objective of this article is to enumerate the problems and then to propose an accurate and robust numerical solution algorithm. A discrete scheme and a numerical solution algorithm for the Landau–Lifshitz equation are described. A nonlinear multigrid method is used for handling the nonlinearities of the resulting discrete system of equations at each time step. We show numerically that the proposed scheme has a second-order convergence in space and time.

© 2010 Elsevier B.V. All rights reserved.

### 1. Introduction

The relaxation process of the magnetization distribution in a ferromagnetic material is described by the Landau–Lifshitz (LL) equation [1,2]. Numerical analysis has played an important role in the investigation of various issues in ferromagnetic materials [3–6]. Recent developments in modeling, analysis, and numerics of ferromagnetism were discussed in survey articles [7,8]. In this paper, we consider the gyromagnetic term in the Landau–Lifshitz equation with a forcing

$$\frac{\partial \mathbf{m}(\mathbf{x}, t)}{\partial t} = -\mathbf{m}(\mathbf{x}, t) \times \Delta \mathbf{m}(\mathbf{x}, t) + \mathbf{f}(\mathbf{x}, t), \quad \mathbf{x} \in \Omega, \quad 0 < t \leq T, \quad (1)$$

where  $\mathbf{m}(\mathbf{x}, t) = (u(\mathbf{x}, t), v(\mathbf{x}, t), w(\mathbf{x}, t))$  is a magnetization vector field and  $\Omega \subset \mathbb{R}^d$  ( $d = 1, 2, 3$ ) is a domain. At the domain boundary  $\partial\Omega$ , we will use either homogeneous Neumann or periodic boundary condition. It is obvious that Eq. (1) with  $\mathbf{f} \equiv 0$  has a length-preserving property during the evolution process. To see this, we do scalar multiplication of Eq. (1) with  $\mathbf{m}$ .

$$\frac{\partial \mathbf{m}}{\partial t} \cdot \mathbf{m} = -(\mathbf{m} \times \Delta \mathbf{m}) \cdot \mathbf{m} = 0. \quad (2)$$

Then,  $\partial|\mathbf{m}|^2/\partial t = 0$ , which implies  $|\mathbf{m}(\mathbf{x}, t)|$  is constant for all  $t$  and each  $\mathbf{x}$ . And we assume that  $|\mathbf{m}(\mathbf{x}, 0)| = 1$ . Let  $E(\mathbf{m}(\mathbf{x}, t))$  be an energy defined by  $E(\mathbf{m}(t)) := \|\nabla \mathbf{m}(t)\|_{L^2(\Omega)}^2$ . By taking an inner product of Eq. (1) with  $\Delta \mathbf{m}$ , we obtain

$$\frac{\partial \mathbf{m}}{\partial t} \cdot \Delta \mathbf{m} = -(\mathbf{m} \times \Delta \mathbf{m}) \cdot \Delta \mathbf{m} = 0. \quad (3)$$

\* Corresponding author.

E-mail address: [cfdkim@korea.ac.kr](mailto:cfdkim@korea.ac.kr) (J. Kim).

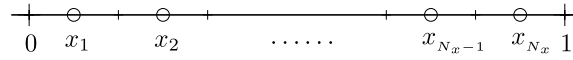


Fig. 1. Cell centered grid.

Using homogeneous Neumann or periodic boundary conditions, from Eq. (3) we have

$$\begin{aligned}
 0 &= \int_{\Omega} \frac{\partial \mathbf{m}}{\partial t} \cdot \Delta \mathbf{m} \, dx = \int_{\partial \Omega} \frac{\partial \mathbf{m}}{\partial t} \cdot \frac{\partial \mathbf{m}}{\partial \mathbf{n}} \, ds - \int_{\Omega} \nabla \cdot \frac{\partial \mathbf{m}}{\partial t} : \nabla \mathbf{m} \, dx \\
 &= -\frac{1}{2} \frac{dE(\mathbf{m}(t))}{dt},
 \end{aligned}
 \tag{4}$$

which implies that  $E(\mathbf{m}(t))$  is constant and this problem has an energy conservation property. Here,  $\mathbf{n}$  is a unit normal vector to  $\partial \Omega$  and the operator ‘:’ is defined as  $A : B = \sum_{ij} a_{ij} b_{ij}$ .

The Crank–Nicolson (CN) scheme is a popular implicit method for solving partial differential equations with second-order accuracy in time and space [9]. However, the method does not always produce accurate results when it is applied to the Landau–Lifshitz equation. It is the objective of this article to enumerate the problems and then to propose an accurate and robust numerical solution algorithm. One- and two-dimensional discrete schemes for the discretized Landau–Lifshitz equation with an exact solution are described and numerically solved using a nonlinear multigrid method. Also, we show that the proposed scheme has a second-order convergence in space and time numerically.

The paper is organized as follows. In Section 2, we describe the discrete scheme of Landau–Lifshitz equation. And we present the nonlinear multigrid method for the discrete system. In Section 3, the numerical results showing performance of the proposed scheme are given. Conclusions are made in Section 4.

## 2. Crank–Nicolson method

### 2.1. Discretization

For simplicity of presentation, we will describe spatial and temporal discretizations of the governing equation in one-dimensional space. Two- and three-dimensional spaces are straightforward extensions. Let us first discretize the given computational domain  $\Omega = (0, 1)$  as a uniform grid with the number of grid points  $N_x$ , a space step  $h = 1/N_x$ , and a time step  $\Delta t = T/N_t$ . Let us denote the numerical approximation of the solution by

$$\begin{aligned}
 \mathbf{m}_i^n &= \mathbf{m}(x_i, t^n) = (u_i^n, v_i^n, w_i^n) \\
 &= (u((i - 0.5)h, n\Delta t), v((i - 0.5)h, n\Delta t), w((i - 0.5)h, n\Delta t)),
 \end{aligned}$$

where  $i = 1, \dots, N_x$  and  $n = 0, 1, \dots, N_t$ . We use a cell centered discretization. See Fig. 1.

Neumann boundary condition is  $\mathbf{m}_x(0, t) = \mathbf{m}_x(1, t) = 0$ . Therefore, we put the  $\mathbf{m}_0 = \mathbf{m}_1$  and  $\mathbf{m}_{N_x+1} = \mathbf{m}_{N_x}$  as the boundary condition. The Crank–Nicolson scheme is given as

$$\frac{\mathbf{m}^{n+1} - \mathbf{m}^n}{\Delta t} = -\frac{\mathbf{m}^{n+1} + \mathbf{m}^n}{2} \times \Delta_h \frac{\mathbf{m}^{n+1} + \mathbf{m}^n}{2} + \mathbf{f}^{n+\frac{1}{2}},
 \tag{5}$$

where  $\Delta_h$  is the standard discretization of  $\Delta$ :

$$\Delta_h \mathbf{m}_i = \frac{1}{h^2} (\mathbf{m}_{i+1} - 2\mathbf{m}_i + \mathbf{m}_{i-1}).$$

Let  $E_h(\mathbf{m}^n)$  be the discrete energy defined by

$$\begin{aligned}
 E_h(\mathbf{m}^n) &= \frac{1}{h} \sum_{i=1}^{N_x} \left[ (u_{i+1}^n - u_i^n)^2 + (v_{i+1}^n - v_i^n)^2 + (w_{i+1}^n - w_i^n)^2 \right] \\
 &= \frac{1}{h} \sum_{i=1}^{N_x} [|\mathbf{m}_{i+1}^n - \mathbf{m}_i^n|^2].
 \end{aligned}$$

We note that in [10] established a weak convergence of the approximate solutions to weak solutions of the Landau–Lifshitz equation.

### 2.2. Properties of the scheme

First, we show that the scheme (5) conserves the magnitude of magnetization.

$$\frac{\mathbf{m}^{n+1} - \mathbf{m}^n}{\Delta t} = -\mathbf{m}^{n+\frac{1}{2}} \times \Delta_h \mathbf{m}^{n+\frac{1}{2}}.
 \tag{6}$$

Taking an inner product of Eq. (6) with  $\mathbf{m}^{n+1} + \mathbf{m}^n$ , we obtain

$$\frac{\mathbf{m}^{n+1} - \mathbf{m}^n}{\Delta t} \cdot (\mathbf{m}^{n+1} + \mathbf{m}^n) = - \left( \mathbf{m}^{n+\frac{1}{2}} \times \Delta_h \mathbf{m}^{n+\frac{1}{2}} \right) \cdot (\mathbf{m}^{n+1} + \mathbf{m}^n) = 0,$$

hence

$$|\mathbf{m}^{n+1}|^2 = |\mathbf{m}^n|^2. \tag{7}$$

Second, we show that the discrete energy is conserved. Forming an inner product between Eq. (6) and  $\Delta_h(\mathbf{m}^{n+1} + \mathbf{m}^n)$ , we obtain

$$\frac{\mathbf{m}^{n+1} - \mathbf{m}^n}{\Delta t} \cdot \Delta_h(\mathbf{m}^{n+1} + \mathbf{m}^n) = - \left( \mathbf{m}^{n+\frac{1}{2}} \times \Delta_h \mathbf{m}^{n+\frac{1}{2}} \right) \cdot \Delta_h(\mathbf{m}^{n+1} + \mathbf{m}^n) = 0.$$

It follows that

$$(\mathbf{m}^{n+1} - \mathbf{m}^n) \cdot \Delta_h(\mathbf{m}^{n+1} + \mathbf{m}^n) = 0. \tag{8}$$

Summation Eq. (8) over  $i = 1, \dots, N_x$  leads to

$$\sum_{i=1}^{N_x} (\mathbf{m}_i^{n+1} - \mathbf{m}_i^n) \cdot \Delta_h(\mathbf{m}_i^{n+1} + \mathbf{m}_i^n) = 0. \tag{9}$$

Using Eq. (7) and periodic boundary condition, Eq. (9) becomes

$$\sum_{i=1}^{N_x} (2\mathbf{m}_i^{n+1} \cdot \mathbf{m}_{i+1}^{n+1} - 2\mathbf{m}_i^n \cdot \mathbf{m}_{i+1}^n) = 0. \tag{10}$$

Now, we get the following energy conservation:

$$\begin{aligned} E(\mathbf{m}^{n+1}) - E(\mathbf{m}^n) &= \frac{1}{h} \sum_{i=1}^{N_x} (|\mathbf{m}_{i+1}^{n+1} - \mathbf{m}_i^{n+1}|^2 - |\mathbf{m}_{i+1}^n - \mathbf{m}_i^n|^2) \\ &= \frac{1}{h} \sum_{i=1}^{N_x} (|\mathbf{m}_{i+1}^{n+1}|^2 - |\mathbf{m}_{i+1}^n|^2 + |\mathbf{m}_i^{n+1}|^2 - |\mathbf{m}_i^n|^2 - 2\mathbf{m}_i^{n+1} \cdot \mathbf{m}_{i+1}^{n+1} + 2\mathbf{m}_i^n \cdot \mathbf{m}_{i+1}^n) = 0, \end{aligned}$$

where we have used Eqs. (7) and (10).

Finally, we show that the truncation error of the scheme is second order in time and space. Let  $u, v, w$  be the exact solution of the partial differential equation (1) without a forcing term. Then, the local truncation error of the first component of the equations is

$$\begin{aligned} T_i^{n+\frac{1}{2}} &= \frac{u_i^{n+1} - u_i^n}{\Delta t} + \frac{v_i^{n+1} + v_i^n}{2} \Delta_h \left( \frac{w_i^{n+1} + w_i^n}{2} \right) - \frac{w_i^{n+1} + w_i^n}{2} \Delta_h \left( \frac{v_i^{n+1} + v_i^n}{2} \right) \\ &= (u_t)_i^{n+\frac{1}{2}} + O(\Delta t^2) + \left( v_i^{n+\frac{1}{2}} + O(\Delta t^2) \right) \left( (w_{xx})_i^{n+\frac{1}{2}} + O(h^2) + O(\Delta t^2) \right) \\ &\quad - \left( w_i^{n+\frac{1}{2}} + O(\Delta t^2) \right) \left( (v_{xx})_i^{n+\frac{1}{2}} + O(h^2) + O(\Delta t^2) \right) \\ &= (u_t + vw_{xx} - wv_{xx})_i^{n+\frac{1}{2}} + O(h^2) + O(\Delta t^2). \end{aligned}$$

Since  $u, v, w$  is the solution of the differential equation so

$$(u_t + vw_{xx} - wv_{xx})_i^{n+\frac{1}{2}} = 0.$$

Therefore, the principal part of the local truncation error is

$$T_i^{n+\frac{1}{2}} = O(h^2) + O(\Delta t^2).$$

For the second and third components of the equations, we get same results.

### 2.3. Solving the nonlinear system—a nonlinear multigrid method

Multigrid methods are generally accepted as among the fastest numerical methods for solving these types of partial differential equations. Since the scheme (5) is nonlinear, we use a nonlinear full approximation storage (FAS) multigrid

method to solve the nonlinear discrete system (5) at the implicit time level. A pointwise Gauss–Seidel relaxation scheme is used as the smoother in the multigrid method. See the reference text [11] for additional details and background. The algorithm of the nonlinear multigrid method for solving the discrete equation is: First, let us rewrite Eq. (5) as

$$N(\mathbf{m}^{n+1}) = \phi^n, \tag{11}$$

where the nonlinear system operator ( $N$ ) is defined as

$$N(\mathbf{m}^{n+1}) = \mathbf{m}^{n+1} + \frac{\Delta t}{2} (\mathbf{m} \times \Delta_h \mathbf{m})^{n+1}$$

and the source term is

$$\phi^n = \mathbf{m}^n - \frac{\Delta t}{2} (\mathbf{m} \times \Delta_h \mathbf{m})^n + \Delta t \mathbf{f}^{n+\frac{1}{2}}.$$

In the following description of one FAS cycle, we assume that a sequence of grids  $\Omega_k$  ( $\Omega_{k-1}$  is coarser than  $\Omega_k$  by factor 2). Given the number  $\beta$  of pre- and post-smoothing relaxation sweeps, an iteration step for the nonlinear multigrid method using the V-cycle is formally written as follows [11]:

*FAS multigrid cycle*

$$\mathbf{m}^{m+1,k} = \text{FAScycle}(k, \mathbf{m}^{m,k}, N_k, \phi^{n,k}, \beta).$$

That is,  $\mathbf{m}^{m,k}$  and  $\mathbf{m}^{m+1,k}$  are the approximation of  $\mathbf{m}^{n+1,k}$  before and after an FAScycle. If  $\Omega_k$  is the finest mesh and  $\|\mathbf{m}^{m+1,k} - \mathbf{m}^{m,k}\|_\infty < \text{tol}$ , then we let  $\mathbf{m}^{n+1} = \mathbf{m}^{m+1,k}$ . Now, we define the FAScycle.

*Step (1) Pre-smoothing*

$$\bar{\mathbf{m}}^{m,k} = \text{SMOOTH}^\beta(\mathbf{m}^{m,k}, N_k, \phi^{n,k}), \tag{12}$$

which means performing  $\beta$  smoothing steps with the initial approximation  $\mathbf{m}^{m,k}$ , source term  $\phi^{n,k}$ , and SMOOTH relaxation operator to get the approximation  $\bar{\mathbf{m}}^{m,k}$ . In its component form, Eq. (11) becomes

$$\begin{pmatrix} u_i^{n+1} \\ v_i^{n+1} \\ w_i^{n+1} \end{pmatrix} + \frac{\Delta t}{2} \begin{pmatrix} v_i \Delta_h w_i - w_i \Delta_h v_i \\ w_i \Delta_h u_i - u_i \Delta_h w_i \\ u_i \Delta_h v_i - v_i \Delta_h u_i \end{pmatrix}^{n+1} = \phi_i^n \quad \text{for } i = 1, \dots, N_x. \tag{13}$$

The main idea of the proposed scheme is a cancelation. Note that

$$\begin{aligned} v_i \Delta_h w_i - w_i \Delta_h v_i &= v_i \frac{w_{i-1} - 2w_i + w_{i+1}}{h^2} - w_i \frac{v_{i-1} - 2v_i + v_{i+1}}{h^2} \\ &= v_i \frac{w_{i-1} + w_{i+1}}{h^2} - w_i \frac{v_{i-1} + v_{i+1}}{h^2} \\ &= v_i \tilde{\Delta}_h w_i - w_i \tilde{\Delta}_h v_i \quad \text{for } i = 1, \dots, N_x, \end{aligned} \tag{14}$$

where  $\tilde{\Delta}_h w_i = (w_{i-1} + w_{i+1})/h^2$ . Similarly, we have

$$w_i \Delta_h u_i - u_i \Delta_h w_i = w_i \tilde{\Delta}_h u_i - u_i \tilde{\Delta}_h w_i, \tag{15}$$

$$u_i \Delta_h v_i - v_i \Delta_h u_i = u_i \tilde{\Delta}_h v_i - v_i \tilde{\Delta}_h u_i. \tag{16}$$

This cancelation stabilizes the scheme. By Eqs. (14), (15) and (16) we rewrite the above equation.

$$A_i \begin{pmatrix} u_i^{n+1} \\ v_i^{n+1} \\ w_i^{n+1} \end{pmatrix} = \begin{pmatrix} \alpha_i \\ \beta_i \\ \gamma_i \end{pmatrix},$$

where

$$A_i = \begin{pmatrix} 1 & \frac{\Delta t}{2} \tilde{\Delta}_h w_i^{n+1} & -\frac{\Delta t}{2} \tilde{\Delta}_h v_i^{n+1} \\ -\frac{\Delta t}{2} \tilde{\Delta}_h w_i^{n+1} & 1 & \frac{\Delta t}{2} \tilde{\Delta}_h u_i^{n+1} \\ \frac{\Delta t}{2} \tilde{\Delta}_h v_i^{n+1} & -\frac{\Delta t}{2} \tilde{\Delta}_h u_i^{n+1} & 1 \end{pmatrix} = \begin{pmatrix} 1 & c & -b \\ -c & 1 & a \\ b & -a & 1 \end{pmatrix}$$

and  $(\alpha_i, \beta_i, \gamma_i)^T$  is the right-hand side term in Eq. (13). Then using Cramer’s rule, we obtain

$$(u_i^{n+1}, v_i^{n+1}, w_i^{n+1}) = 1/|A_i|(|A_{i,1}|, |A_{i,2}|, |A_{i,3}|), \quad i = 1, \dots, N_x$$

where  $A_{i,j}$  is obtained by replacing the  $j$ th column of  $A_i$  with  $(\alpha_i, \beta_i, \gamma_i)^T$ .

$$\begin{aligned} |A_i| &= 1 + a^2 + b^2 + c^2, \\ |A_{i,1}| &= \alpha_i(1 + a^2) - \beta_i(c - ab) + \gamma_i(ac + b), \\ |A_{i,2}| &= \alpha_i(ab + c) + \beta_i(1 + b^2) - \gamma_i(a - bc), \\ |A_{i,3}| &= \alpha_i(ac - b) + \beta_i(a + bc) + \gamma_i(1 + c^2). \end{aligned}$$

We can rewrite Eq. (11) as a matrix form:

$$\begin{pmatrix} 1 & c & -b \\ -c & 1 & a \\ b & -a & 1 \end{pmatrix} \mathbf{m}_i^{n+1} = \Phi_i^n, \tag{17}$$

where

$$a = \frac{\Delta t}{2} \tilde{\Delta}_h u_i^{n+1}, \quad b = \frac{\Delta t}{2} \tilde{\Delta}_h v_i^{n+1}, \quad \text{and} \quad c = \frac{\Delta t}{2} \tilde{\Delta}_h w_i^{n+1}.$$

To derive a Gauss–Seidel type iteration, we replace  $\mathbf{m}_\alpha^{n+1}$  in Eq. (17) with  $\bar{\mathbf{m}}_\alpha^{m,k}$  if  $\alpha \leq i$ , otherwise with  $\mathbf{m}_\alpha^{m,k}$ , i.e.,

$$\begin{pmatrix} 1 & c & -b \\ -c & 1 & a \\ b & -a & 1 \end{pmatrix} \bar{\mathbf{m}}_i^{m,k} = \Phi_i^n, \tag{18}$$

where

$$a = \frac{\Delta t}{2} \frac{\bar{u}_{i-1,j}^{m,k} + u_{i+1,j}^{m,k}}{h^2}, \quad b = \frac{\Delta t}{2} \frac{\bar{v}_{i-1,j}^{m,k} + v_{i+1,j}^{m,k}}{h^2}, \quad c = \frac{\Delta t}{2} \frac{\bar{w}_{i-1,j}^{m,k} + w_{i+1,j}^{m,k}}{h^2}.$$

**Step (2) Coarse grid correction**

- Compute the defect:  $\bar{\mathbf{d}}^{m,k} = \Phi^{n,k} - N_k(\bar{\mathbf{m}}^{m,k})$ .
  - Restrict the defect and  $\bar{\mathbf{m}}^{m,k} : \bar{\mathbf{d}}^{m,k-1} = I_k^{k-1}(\bar{\mathbf{d}}^{m,k})$ ,  $\bar{\mathbf{m}}^{m,k-1} = I_k^{k-1}(\bar{\mathbf{m}}^{m,k})$ .
- The restriction operator  $I_k^{k-1}$  maps  $k$ -level functions to  $(k - 1)$ -level functions.

$$d^{k-1}(x_i, y_j) = I_k^{k-1} d^k(x_i, y_j) = \frac{1}{4} \left[ d^k(x_{i-\frac{1}{2}}, y_{j-\frac{1}{2}}) + d^k(x_{i-\frac{1}{2}}, y_{j+\frac{1}{2}}) + d^k(x_{i+\frac{1}{2}}, y_{j-\frac{1}{2}}) + d^k(x_{i+\frac{1}{2}}, y_{j+\frac{1}{2}}) \right].$$

- Compute the right-hand side:  $\Phi^{n,k-1} = \bar{\mathbf{d}}^{m,k-1} + N_{k-1}(\bar{\mathbf{m}}^{m,k-1})$ .
- Compute an approximate solution  $\hat{\mathbf{m}}^{m,k-1}$  of the coarse grid equation on  $\Omega_{k-1}$ , i.e.

$$N_{k-1}(\hat{\mathbf{m}}^{m,k-1}) = \Phi^{n,k-1}. \tag{19}$$

If  $k = 1$ , we apply the smoothing procedure in (12) to obtain the approximate solution. If  $k > 1$ , we solve (19) by performing a FAS  $k$ -grid cycle using  $\bar{\mathbf{m}}^{m,k-1}$  as an initial approximation:

$$\hat{\mathbf{m}}^{m,k-1} = \text{FAScycle}(k - 1, \bar{\mathbf{m}}^{m,k-1}, N_{k-1}, \Phi^{n,k-1}, \beta).$$

- Compute the coarse grid correction (CGC):  $\hat{\mathbf{v}}^{m,k-1} = \hat{\mathbf{m}}^{m,k-1} - \bar{\mathbf{m}}^{m,k-1}$ .
- Interpolate the correction:  $\hat{\mathbf{v}}^{m,k} = I_{k-1}^k \hat{\mathbf{v}}^{m,k-1}$ .
- Compute the corrected approximation on  $\Omega_k$ :  $\mathbf{m}^{m,\text{after CGC},k} = \bar{\mathbf{m}}^{m,k} + \hat{\mathbf{v}}^{m,k}$ .

**Step (3) Post-smoothing:**  $\mathbf{m}^{m+1,k} = \text{SMOOTH}^\beta(\mathbf{m}^{m,\text{after CGC},k}, N_k, \Phi^{n,k})$ . This completes the description of a nonlinear FAScycle. After we get a solution after one FAScycle, using an updated source term, we repeatedly perform iterations until the numerical solution converges.

Now we consider the scheme with no cancellation. We rewrite Eq. (13).

$$A_i \begin{pmatrix} u_i^{n+1} \\ v_i^{n+1} \\ w_i^{n+1} \end{pmatrix} = \Phi_i^n \quad \text{for } i = 1, \dots, N_x.$$

To discuss the stability of the Crank–Nicolson scheme, we compute the characteristic polynomial of  $A_i$ .

$$\det(A_i - \lambda I) = (1 - \lambda)^3 + (1 - \lambda)(a^2 + b^2 + c^2).$$

The three eigenvalues of  $A_i$  are

$$\lambda_1 = 1, \quad \lambda_2 = 1 + i\sqrt{a^2 + b^2 + c^2}, \quad \text{and} \quad \lambda_3 = 1 - i\sqrt{a^2 + b^2 + c^2}.$$

Thus, the three eigenvalues of  $A_i^{-1}$  are

$$\gamma_1 = 1/\lambda_1, \quad \gamma_2 = 1/\lambda_2, \quad \text{and} \quad \gamma_3 = 1/\lambda_3.$$

The absolute values of three eigenvalues of  $A_i^{-1}$  are

$$|\gamma_1| = 1, \quad |\gamma_2| = |\gamma_3| = \frac{1}{\sqrt{1 + a^2 + b^2 + c^2}} \leq 1.$$

Without cancelation,  $a, b,$  and  $c$  are small compared to 1, on the other hand, with cancelation  $a^2 + b^2 + c^2 \approx O(1/h^4)$ . Therefore,  $1/\sqrt{1 + a^2 + b^2 + c^2} \approx O(h^2) \ll 1$  and this makes the iterations stable.

### 3. Numerical results

In this section we perform numerical experiments with exact solutions to verify the second-order accuracy of the proposed scheme in time and space. Without the forcing term, we also show the energy conservation property.

#### 3.1. One space dimension

##### 3.1.1. Convergence test

We consider one-dimensional Landau–Lifshitz equation with a source:

$$\mathbf{m}_t = -\mathbf{m} \times \mathbf{m}_{xx} + \mathbf{f} \quad \text{on } \Omega = (0, 1). \tag{20}$$

An exact solution of Eq. (20) is

$$\mathbf{m}^e = \begin{pmatrix} u^e \\ v^e \\ w^e \end{pmatrix} = \begin{pmatrix} \cos(x^2(1-x)^2) \sin(t) \\ \sin(x^2(1-x)^2) \sin(t) \\ \cos(t) \end{pmatrix}.$$

In its component form, the forcing term  $\mathbf{f} = \mathbf{m}_t^e + \mathbf{m}^e \times \mathbf{m}_{xx}^e$  can be calculated as follows.

$$\mathbf{f} = \begin{pmatrix} \cos(X) \cos(t) + [(X')^2 \sin(X) - X'' \cos(X)] \sin(t) \cos(t) \\ \sin(X) \cos(t) - [(X')^2 \cos(X) + X'' \sin(X)] \sin(t) \cos(t) \\ -\sin(t) + X'' \sin^2(t) \end{pmatrix},$$

where  $X = x^2(1-x)^2$ . Now, we will solve Eq. (20) with an initial condition  $\mathbf{m}(x, 0) = (0, 0, 1)$  and zero Neumann boundary condition; i.e.,  $\mathbf{m}_x = \mathbf{0}$  at  $\partial\Omega = \{0, 1\}$ . We define the numerical error  $\mathbf{e}_i^n = \mathbf{m}_i^n - \mathbf{m}^e(x_i, t^n)$  for  $i = 1, 2, \dots, N_x$ . The discrete  $l_2$ -norm and the maximum norm are defined as

$$\|\mathbf{e}^n\|_{l_2} = \sqrt{\sum_{1 \leq i \leq N_x} \frac{\mathbf{e}_i^n \cdot \mathbf{e}_i^n}{3N_x}} \quad \text{and} \quad \|\mathbf{e}^n\|_{\infty} = \max_{1 \leq i \leq N_x} \sqrt{\mathbf{e}_i^n \cdot \mathbf{e}_i^n}.$$

To obtain an estimate of the convergence rate, we performed a number of simulations on a set of increasingly finer grids. We computed the numerical solutions on uniform grids,  $h = 1/2^n$  for  $n = 6, 7, 8, 9$  and  $10$ . For each case, we ran the calculation to time  $T = 1$  with a time step  $\Delta t = 0.32$  h. Fig. 2 shows the numerical results for the one-dimensional equation: (a)  $u$ , (b)  $v$ , (c)  $w$ , and (d)  $\mathbf{m}$  at  $T = 1$ . The numerical results agree very well with the exact solution. The errors and rates of convergence are given in Table 1. The results suggest that the scheme is indeed second-order accurate in space and time. Also, the convergence results imply the preservation of the length of the vector field,  $\mathbf{m}$ .

We calculate the stability constraint for the proposed scheme and take a similar test problem in [12]. We try to find the maximum  $\Delta t$  corresponding to different spatial grid sizes  $h$  so that stable solutions can be computed up to  $T = 1$ . The results are shown in Table 2 and we obtain stable solutions for all five mesh sizes. The results indicate that the proposed CN scheme is practically unconditionally stable because time step constraint from accuracy concern is more restrictive than one from stability of the numerical scheme.

##### 3.1.2. Energy conservation

Next, we investigate the energy conservation property when  $\mathbf{f} \equiv \mathbf{0}$ . An exact solution of the equation is

$$\begin{aligned} u^e(x, t) &= \sin(\alpha) \cos(kx + tk^2 \cos(\alpha)), \\ v^e(x, t) &= \sin(\alpha) \sin(kx + tk^2 \cos(\alpha)), \\ w^e(x, t) &= \cos(\alpha). \end{aligned}$$

We see that the function  $\mathbf{m}(x, t) = (u^e(x, t), v^e(x, t), w^e(x, t))$  satisfies Eq. (1). Now we apply an initial condition to Eq. (1)

$$(u_0, v_0, w_0) = (\sin(\alpha) \cos(kx), \sin(\alpha) \sin(kx), \cos(\alpha)),$$

where  $\alpha = \pi/4, k = 2\pi$ , and a periodic boundary condition is applied; i.e.,  $\mathbf{m}_0 = \mathbf{m}_{N_x}$  and  $\mathbf{m}_{N_x+1} = \mathbf{m}_1$ .

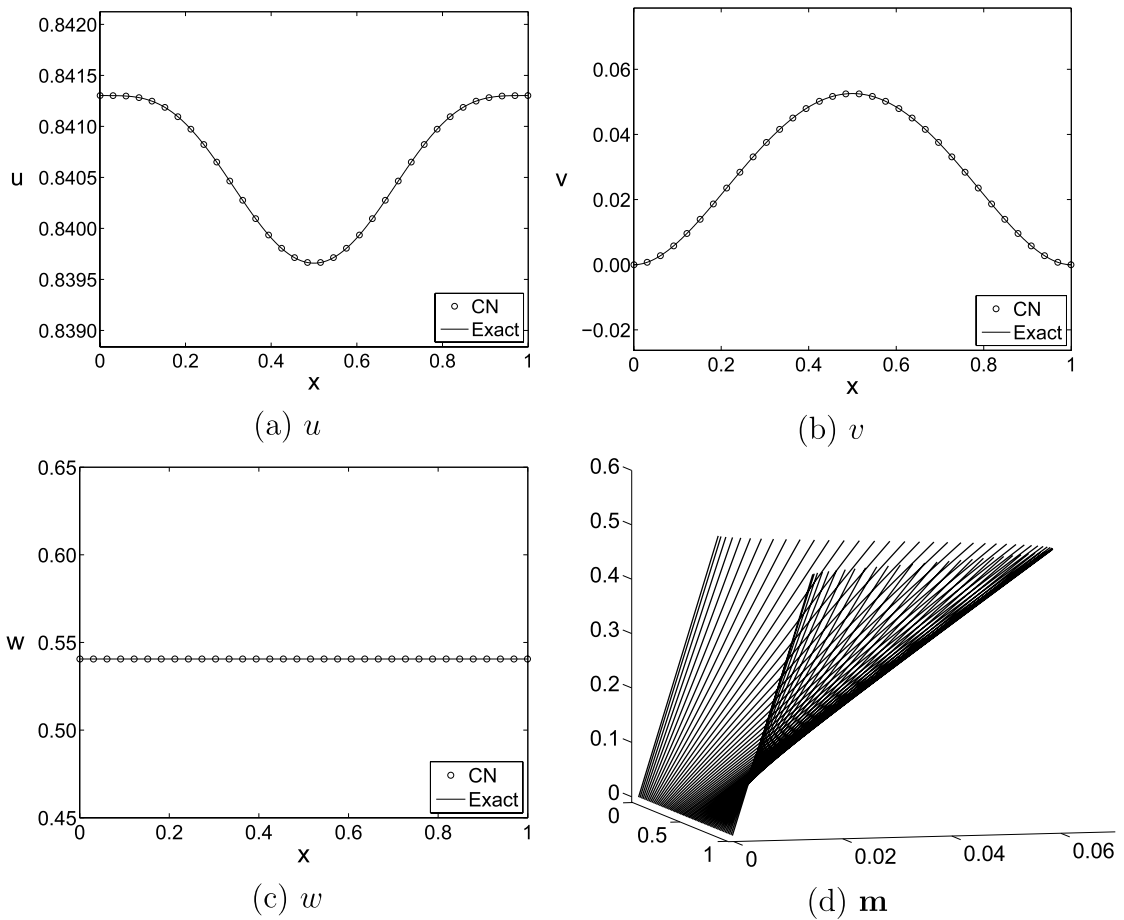


Fig. 2. Magnetization distribution for one-dimensional equation: (a)  $u$ , (b)  $v$ , (c)  $w$ , and (d)  $\mathbf{m}$  at  $T = 1$ .

Table 1

The  $l_2$  and maximum norms and convergence rates with space step  $h = 1/N_x$ , time step  $\Delta t = 0.32$  h, total time  $T = 1$ , and an iteration convergence tolerance of  $10^{-10}$ .

Case	64	Rate	128	Rate	256	Rate	512	Rate	1024
$\ \mathbf{e}^n\ _{l_2}$	6.5E-5	1.99	1.6E-5	1.99	4.1E-6	2.00	1.0E-6	2.00	2.5E-7
$\ \mathbf{e}^n\ _{\infty}$	1.1E-4	1.99	2.7E-5	1.99	6.7E-6	2.00	1.7E-6	1.99	4.2E-7

Table 2

Stability constraint of  $\Delta t$  for the proposed scheme.

Mesh size	$h = 1/64$	$h = 1/128$	$h = 1/256$	$h = 1/512$	$h = 1/1024$
Time step	$\Delta t \geq h$	$\Delta t \geq h$	$\Delta t \geq h$	$\Delta t \geq h$	$\Delta t \geq h$

Table 3

The  $l_2$  and maximum norms and convergence rates with space step  $h = 1/N_x$ , time step  $\Delta t = 0.32$  h, total time  $T = 1$ , and an iteration convergence tolerance of  $10^{-10}$ .

Case	64	Rate	128	Rate	256	Rate	512	Rate	1024
$\ \mathbf{e}^n\ _{l_2}$	2.8E-2	1.98	6.9E-3	1.99	1.7E-3	1.99	4.3E-4	1.99	1.1E-4
$\ \mathbf{e}^n\ _{\infty}$	4.8E-2	1.98	1.2E-2	1.99	3.0E-3	1.99	7.5E-4	1.99	1.9E-4

Theoretically, this energy is constant irrespective of time. Now we confirm that numerically. Fig. 3 shows a numerical result for the evolution of the discrete energy up to time  $T = 1$  by the proposed scheme with  $N_x = 64$ ,  $h = 1/N_x$ , and  $\Delta t = 0.32$  h. We can see that the conservation of energy holds. Fig. 4 shows magnetization distribution for one-dimensional equation: (a)  $u$ , (b)  $v$ , (c)  $w$ , and (d)  $\mathbf{m}$  at  $T = 1$  without forcing term and periodic boundary condition.

We also calculated the rate of convergence. The errors and rates of convergence are given in Table 3. The results suggest that the scheme is indeed second-order accurate in space and time.

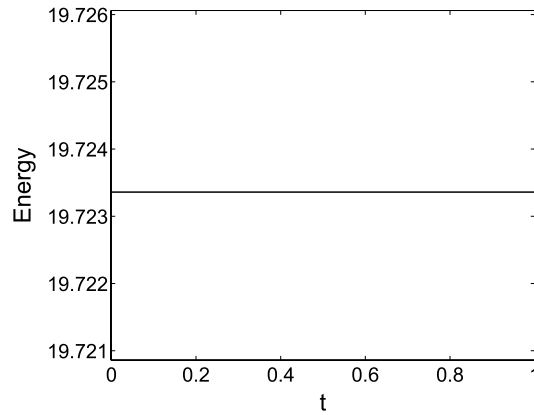
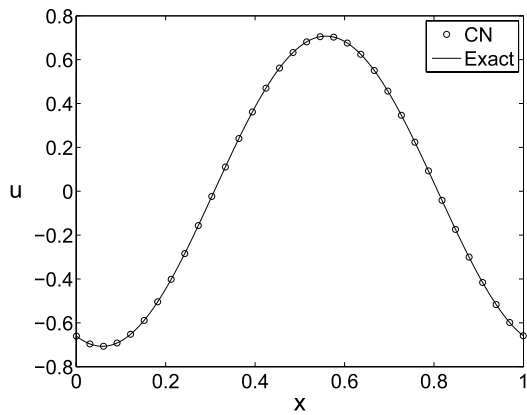
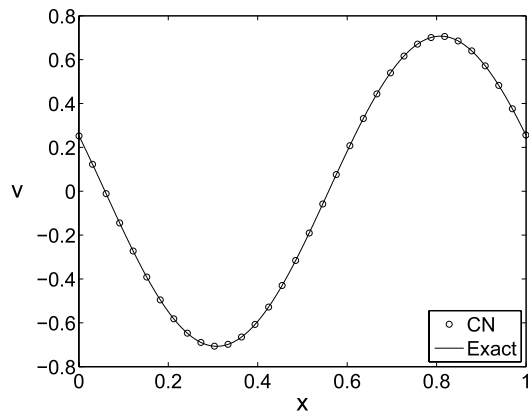


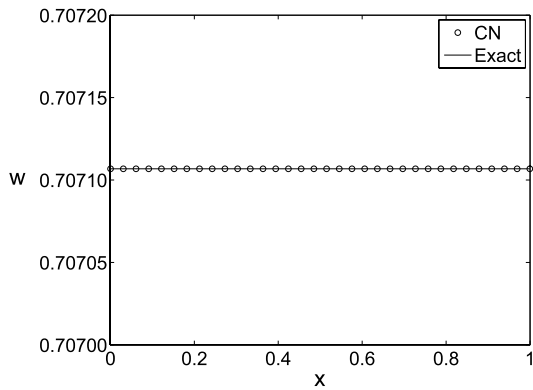
Fig. 3. A temporal evolution of the discrete energy of the numerical solution.



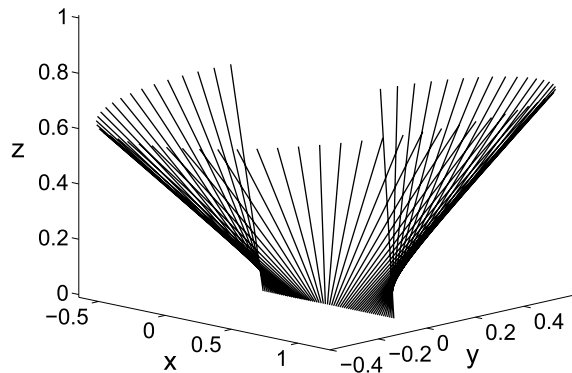
(a)  $u$



(b)  $v$



(c)  $w$



(d)  $m$

Fig. 4. Magnetization distribution for one-dimensional equation: (a)  $u$ , (b)  $v$ , (c)  $w$ , and (d)  $m$  at  $T = 1$  without forcing term and periodic boundary condition.

### 3.2. Two space dimensions

In this section we perform two-dimensional numerical experiments with exact solutions to verify the second-order accuracy of the proposed scheme in time and space. Without the forcing term, we also show the energy conservation property.



**Table 4**

The  $l_2$  and the maximum norms and convergence rates for  $\mathbf{m}$  of CN scheme with space step  $h = 1/N_x$ , time step  $\Delta t = 0.32$  h, total time  $T = 0.01$ , and an iteration convergence tolerance of  $10^{-10}$ .

Case	64 <sup>2</sup>	Rate	128 <sup>2</sup>	Rate	256 <sup>2</sup>	Rate	512 <sup>2</sup>	Rate	1024 <sup>2</sup>
$\ \mathbf{e}^n\ _{l_2}$	6.6E–9	1.99	1.6E–9	1.99	4.1E–10	1.99	1.0E–10	2.00	2.6E–11
$\ \mathbf{e}^n\ _\infty$	1.3E–8	1.99	3.4E–9	1.98	8.4E–10	2.00	2.1E–10	2.00	5.3E–11

3.2.1. Convergence test

The two-dimensional equation on  $\Omega = (0, 1) \times (0, 1)$  with zero Neumann boundary conditions is considered. An exact solution is

$$\mathbf{m}^e = \begin{pmatrix} u^e \\ v^e \\ w^e \end{pmatrix} = \begin{pmatrix} \cos(x^2(1-x)^2y^2(1-y)^2) \sin(t) \\ \sin(x^2(1-x)^2y^2(1-y)^2) \sin(t) \\ \cos(t) \end{pmatrix}.$$

The forcing term  $\mathbf{f} = (f_1, f_2, f_3) = \mathbf{m}_t^e + \mathbf{m}^e \times \Delta \mathbf{m}^e$  can be calculated as follows.

$$\begin{aligned} f_1 &= \cos(XY) \cos(t) + [(Y^2(X')^2 + X^2(Y')^2) \sin(XY) - (YX'' + XY'')] \sin(t) \cos(t), \\ f_2 &= \sin(XY) \cos(t) - [(Y^2(X')^2 + X^2(Y')^2) \cos(XY) + (YX'' + XY'')] \sin(t) \cos(t), \\ f_3 &= -\sin(t) + (YX'' + XY'') \sin^2(t), \end{aligned}$$

where  $X = x^2(1-x)^2$ ,  $Y = y^2(1-y)^2$ , and prime denotes a derivative of functions with respect to its argument variable. Now, we will solve the following equation with an initial condition  $\mathbf{m}(x, y, 0) = (0, 0, 1)$ .

$$\mathbf{m}_t = -\mathbf{m} \times (\mathbf{m}_{xx} + \mathbf{m}_{yy}) + \mathbf{f} \tag{21}$$

with zero Neumann boundary condition

$$\mathbf{m}_x(0, y, t) = \mathbf{m}_x(1, y, t) = \mathbf{m}_y(x, 0, t) = \mathbf{m}_y(x, 1, t) = \mathbf{0}.$$

We let  $\mathbf{e}_{ij}^n = \mathbf{m}_{ij}^n - \mathbf{m}^e(x_i, y_j, t^n)$  for  $i = 1, 2, \dots, N_x$  and  $j = 1, 2, \dots, N_y$ . The discrete  $l_2$ -norm and the maximum norm are defined as

$$\|\mathbf{e}^n\|_{l_2} = \sqrt{\sum_{1 \leq i \leq N_x} \sum_{1 \leq j \leq N_y} \frac{\mathbf{e}_{ij}^n \cdot \mathbf{e}_{ij}^n}{3N_x N_y}} \quad \text{and} \quad \|\mathbf{e}^n\|_\infty = \max_{1 \leq i \leq N_x} \max_{1 \leq j \leq N_y} \sqrt{\mathbf{e}_{ij}^n \cdot \mathbf{e}_{ij}^n}.$$

We performed a number of simulations on a set of increasingly finer grids to calculate the rate of convergence. The results are shown in Table 4. The  $l_2$  and the maximum norms and convergence rates for  $\mathbf{m}$  of CN scheme with space step  $h = 1/N_x$ , time step  $\Delta t = 0.32$  h, total time  $T = 0.01$ ,  $\alpha = \pi/24$ , and an iteration convergence tolerance of  $10^{-10}$ . The results suggest that the scheme is indeed second-order accurate in space and time.

3.2.2. Energy conservation

We consider Eq. (1) in its component form with the source term  $\mathbf{f} \equiv \mathbf{0}$  on the two-dimensional unit domain. An exact solution of the equation is

$$\begin{aligned} u^e(x, y, t) &= \sin(\alpha) \cos(k(x+y) + 2tk^2 \cos(\alpha)), \\ v^e(x, y, t) &= \sin(\alpha) \sin(k(x+y) + 2tk^2 \cos(\alpha)), \\ w^e(x, y, t) &= \cos(\alpha), \end{aligned}$$

where  $\alpha = \pi/24$ ,  $k = 2\pi$ . We see that the function  $\mathbf{m}(x, y, t) = (u^e(x, y, t), v^e(x, y, t), w^e(x, y, t))$  satisfies Eq. (1). Now we apply an initial conditions to Eq. (1)

$$(u_0, v_0, w_0) = (\sin(\alpha) \cos(k(x+y)), \sin(\alpha) \sin(k(x+y)), \cos(\alpha))$$

and a periodic boundary condition is applied; i.e.,

$$\begin{aligned} \mathbf{m}_{0,j} &= \mathbf{m}_{N_x,j}, & \mathbf{m}_{N_x+1,j} &= \mathbf{m}_{1,j} & \text{for } 1 \leq j \leq N_y, \\ \mathbf{m}_{i,0} &= \mathbf{m}_{i,N_y}, & \mathbf{m}_{i,N_y+1} &= \mathbf{m}_{i,1} & \text{for } 1 \leq i \leq N_x. \end{aligned}$$

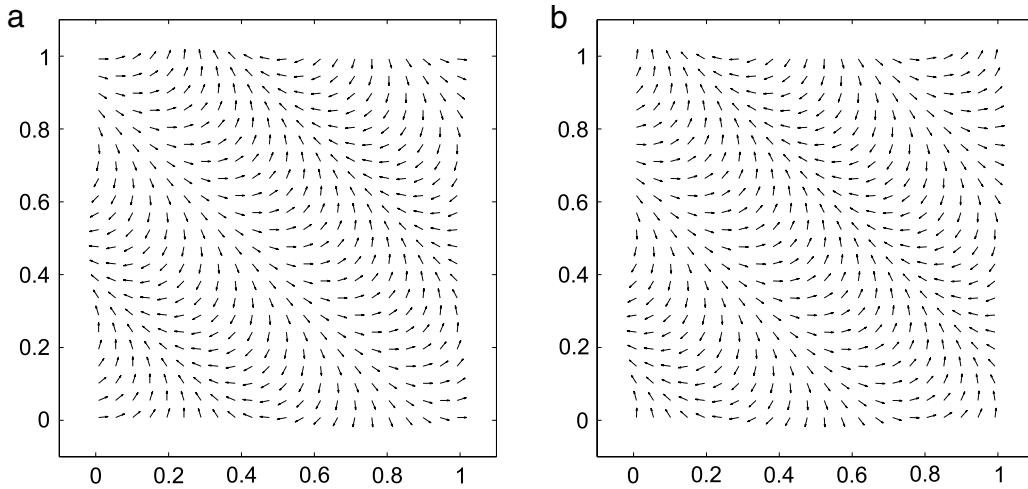
Table 5 shows the  $l_2$  and maximum norms and convergence rates with space step  $h = 1/N_x$ , time step  $\Delta t = 0.32$  h, total time  $T = 0.01$ ,  $\alpha = \pi/24$ , and an iteration convergence tolerance of  $10^{-10}$ . The results suggest that the scheme is second-order accurate in space and time.

Fig. 5 shows the orthogonal projection of the vector field  $0.1\mathbf{m}$  of the numerical solution onto the  $xy$  plane at (a)  $T = 0$  and (b)  $T = 0.1$ . We observe that the solution at  $T = 0.1$  is a translation of the initial configuration without changing its magnitude. Here we scaled  $\mathbf{m}$  as  $0.1\mathbf{m}$  for a visual clarity.

**Table 5**

The  $l_2$  and maximum norms and convergence rates with space step  $h = 1/N_x$ , time step  $\Delta t = 0.32$  h, total time  $T = 0.01$ ,  $\alpha = \pi/24$ , and an iteration convergence tolerance of  $10^{-10}$ .

Case	64 <sup>2</sup>	Rate	128 <sup>2</sup>	Rate	256 <sup>2</sup>	Rate	512 <sup>2</sup>	Rate	1024 <sup>2</sup>
$\ \mathbf{e}^n\ _{l_2}$	7.8E-4	1.97	2.0E-4	1.99	5.0E-5	1.99	1.3E-5	1.99	3.1E-6
$\ \mathbf{e}^n\ _{\infty}$	1.4E-3	1.97	3.4E-4	1.99	8.7E-5	1.99	2.2E-5	1.99	5.4E-6



**Fig. 5.** 2D Landau–Lifshitz equation with periodic boundary condition. (a) initial vector field (b) the numerical solution at  $T = 0.1$ .

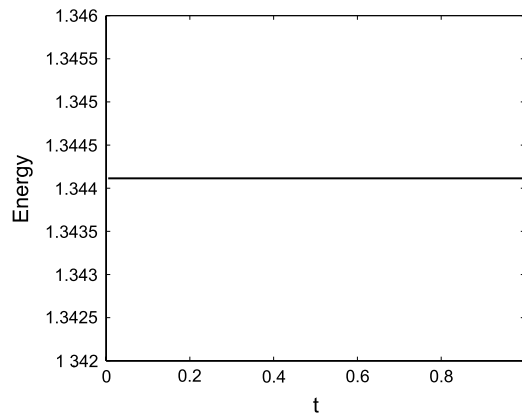


**Fig. 6.** A temporal evolution of the discrete energy of the numerical solution.

Next, we test an energy conservation property. We define a discrete energy as

$$E(\mathbf{m}^n) = \sum_{i=1}^{N_x} \sum_{j=1}^{N_y} \left[ (u_{i+1,j}^n - u_{ij}^n)^2 + (v_{i+1,j}^n - v_{ij}^n)^2 + (w_{i+1,j}^n - w_{ij}^n)^2 + (u_{i,j+1}^n - u_{ij}^n)^2 + (v_{i,j+1}^n - v_{ij}^n)^2 + (w_{i,j+1}^n - w_{ij}^n)^2 \right].$$

Theoretically, this energy is constant irrespective of time. Now we confirm that numerically. Fig. 6 shows the time evolution of the energy  $E(\mathbf{m}^n)$  with  $N_x = N_y = 64$ ,  $h = 1/N_x$ ,  $\Delta t = 0.32$  h,  $T = 0.01$ , and  $\alpha = \pi/24$ . As expected from (4), the energy is constant throughout the evolution.

**4. Conclusion**

In this paper, we have proposed a Crank–Nicolson time stepping procedure for LL equation which has a second-order convergence in time and space. We overcame the difficulties with CN scheme associated with LL equation by a cancelation.

We used a nonlinear multigrid method for handling the nonlinearities of the discrete system at each time step. We validated our numerical algorithm by various numerical experiments. We tested the second-order convergence and an energy conservation of the proposed scheme. We also showed that the time step restriction for the stability is less restrictive than the accuracy. As future research, the full version of Landau–Lifshitz equation will be investigated.

## Acknowledgements

This research was supported by the MKE (The Ministry of Knowledge Economy), Korea, under the ITRC (Information Technology Research Center) support program supervised by the NIPA (National IT Industry Promotion Agency) (NIPA-2009-C1090-0902-0013). This work was supported by National Research Foundation of Korea Grant funded by the Korean Government (2009-0074248).

## References

- [1] W.F. Brown Jr., *Micromagnetics*, John Wiley and Sons, New York, 1963.
- [2] L. Landau, E. Lifshitz, On the theory of the dispersion of magnetic permeability in ferromagnetic bodies, *Phys. Z. Sowjetunion* 8 (1935) 153–169.
- [3] H.N. Bertram, C. Seberino, Numerical simulations of hysteresis in longitudinal magnetic tape, *J. Magn. Magn. Mater.* 193 (1999) 388–394.
- [4] J.L. Blue, M.R. Scheinfein, Using multipoles decreases computation time for magnetic self-energy, *IEEE Trans. Magn.* 27 (1991) 4778–4780.
- [5] J. Fidler, T. Schrefl, Micromagnetic modeling—the current state of the art, *J. Phys. D: Appl. Phys.* 33 (15) (2000) 135–156.
- [6] M. Jones, J.J. Miles, An accurate and efficient 3D micromagnetic simulation of metal evaporated tape, *J. Magn. Magn. Mater.* 171 (1997) 190–208.
- [7] I. Cimrák, A survey on the numerics and computations for the Landau–Lifshitz equation of micromagnetism, *Arch. Comput. Methods Eng.* 15 (3) (2008) 277–309.
- [8] M. Kruzik, A. Prohl, Recent developments in the modeling, analysis, and numerics of ferromagnetism, *SIAM Rev.* 48 (3) (2006) 439–483.
- [9] C. Sun, C.W. Trueman, Unconditionally stable Crank–Nicolson scheme for solving the two-dimensional Maxwell's equations, *IEEE Electron Device Lett.* 39 (2003) 595–597.
- [10] I. Cimrák, Convergence result for the constraint preserving mid-point scheme for micromagnetism, *J. Comput. Appl. Math.* 228 (2009) 238–246.
- [11] U. Trottenberg, C. Oosterlee, A. Schüller, *Multigrid*, Academic Press, New York, 2001.
- [12] X.P. Wang, C.J. Garcia-Cervera, E. Weinan, A Gauss–Seidel projection method for micromagnetics simulations, *J. Comput. Phys.* 171 (2001) 357–372.